Electromagnetic Fields, Field Confinement, and Energy Flow in Dispersionless Single-Mode Lightguides With Graded-Index Profiles

By U. C. PAEK, G. E. PETERSON, and A. CARNEVALE

(Manuscript received February 13, 1981)

It is shown by numerical solution of Maxwell's equations that, for a given wavelength, the degree of confinement of the electromagnetic field to the core of a graded-index, single-mode, optical-fiber can be optimized by the proper choice of the radial variation of the index. Such confinement of the energy to the core helps alleviate loss. The fibers considered have zero total dispersion bandwidths in excess of 100 GHz·Km, at wavelengths between 1.3 µm and 1.55 µm.

I. INTRODUCTION

Our earlier work described a method of designing single-mode lightguides with zero total dispersion by varying the index profile in the core.[1] In the range of wavelengths between 1.3 µm and 1.55 µm, bandwidths in excess of 100 GHz·Km are attainable by balancing material dispersion with waveguide dispersion.[2,3] However, one of the serious difficulties with single-mode fibers is microbending loss. We know that the microbending loss for the case of the step-index, single-mode fiber is proportional to λ^2/Δ^3.[4,5,6] Here, λ refers to the operating wavelength and Δ to the relative index difference which is defined as:

$$\Delta = (N_{\text{core}} - N_{\text{clad}})/N_{\text{core}} . \tag{1}$$

Now the design of a single-mode fiber must be such that it prevents the field of the fundamental mode (HE_{11}) from extending well into the cladding. In other words, the electromagnetic field must be tightly confined to the core. To this end, two methods can be considered: one is to increase Δ, which is a common and prevailing method, and the other is to change the index profile in the core. This work will focus on the latter case by assuming an α index profile, where $N = N_1(1 - \Delta r^\alpha)$. Reducing microbending by profile design might be advantageous be-

cause the TE and TM modes can be maintained well beyond the cutoff point of a step-index, single-mode fiber and the manufacturing tolerances are relaxed. Note that $N_1 = N_{core}$ and $N_2 = N_{clad}$.

For a single-mode lightguide having a radially inhomogeneous core, it is usually not possible to obtain analytical solutions of closed form for Maxwell's equations. Hence, to attain vector electromagnetic field distributions of the HE_{11} mode and to determine accurate propagation characteristics of a single-mode fiber, we used a numerical method to solve the governing equations.[7,8]

II. THEORY

Our method of solving Maxwell's equations for lightguides has been described in our earlier publications. However, we did not consider the cladding fields in much detail. For the work to be described in this paper, this is essential. Thus, we develop the necessary mathematical expressions.

In an optical fiber having a permittivity ϵ and permeability μ, we assume that the outer diameter D is much larger than the core
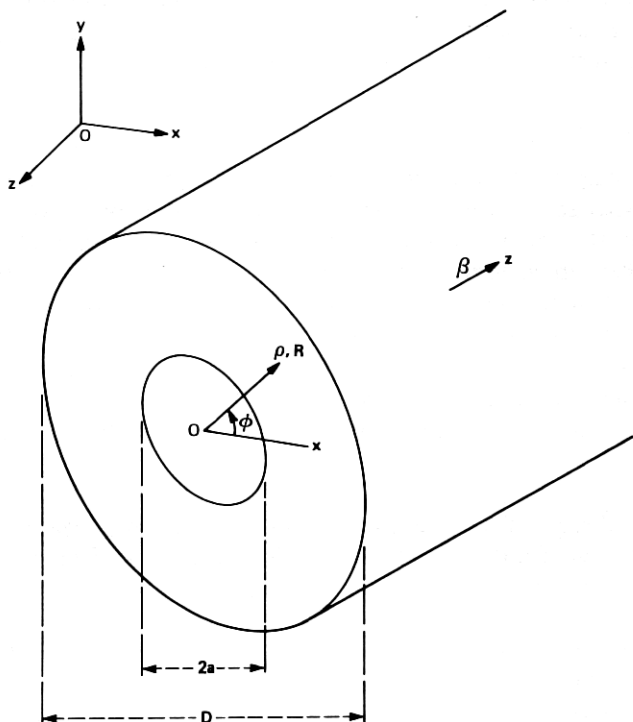

Fig. 1—A cross-section of a fiber and its cylindrical coordinate system.

diameter $2a$. In a cylindrical coordinate system, for a position vector r having as its components $\{R, \phi, z\}$, the corresponding components of electric and magnetic fields can be written as $E = \{E_R, E_\phi, E_z\}$ and $H = \{H_R, H_\phi, H_z\}$ (see Fig. 1). However, in obtaining a complete set of vector solutions, it is only necessary to find the tangential components $\{E_\phi, E_z\}$ and $\{H_\phi, H_z\}$ since the radial components E_R and H_R are linear combinations of the other components. In particular,

$$E_R = -\frac{Z_o}{\rho N^2} H_z + \frac{Z_o N_e}{N^2} H_\phi, \tag{2}$$

$$H_R = \frac{1}{Z_o} E_z - \frac{N_e}{Z_o} E_\phi. \tag{3}$$

In addition, the tangential field components are continuous through the core-cladding interface and this simplifies the mathematics of the boundary value problem.

In the above equation, Z_o is the wave impedance defined by $(\mu/\epsilon)^{1/2}$ and N is the index of refraction and a function of R. The effective refractive index N_e is defined by two quantities, β and k, where β is the propagation constant along the fiber axis and $k = 2\pi/\lambda$; ρ is a dimensionless quantity defined by Rk. The fundamental HE_{11} mode propagates in the fiber when the angular mode number M equals 1. Moreover, $V < V_c$ must be satisfied. Here V is the normalized frequency and V_c is the cutoff frequency for a single-mode propagation. The V value is defined by

$$V = \frac{2\pi a_{\mathrm{opt}}}{\lambda} \sqrt{N_1^2 - N_2^2}. \tag{4}$$

The input data, a_{opt}, is the optimum core radius that will give zero total dispersion for a given α, Δ, and λ.

In the most general case, there are two possible solutions to Maxwell's equations for a guided mode in a lightguide. A general solution will be a sum of these two vector solutions. We introduce variable Γ_i to establish the following relationship with the tangential field vectors $\{E_\phi, E_z\}$ and $\{H_\phi, H_z\}$.

$$\Gamma_i = \begin{Bmatrix} \Gamma_1 \\ \Gamma_2 \\ \Gamma_3 \\ \Gamma_4 \end{Bmatrix} = \begin{Bmatrix} E_z \\ -iZ_o\rho H_\phi \\ \rho E_\phi \\ -iZ_o H_z \end{Bmatrix} \tag{5}$$

From eq. (5) we denote the two solutions in cores Γ_{i1} and Γ_{i2}. Since our earlier work gave a detailed description of the computation of Γ_{i1} and Γ_{i2}, we will avoid repetition of the procedure for the solution in the core region.[1] In the cladding region, the two solutions designated

by Γ_{i3} and Γ_{i4} are given by the following expressions:[7]

$$\Gamma_{i3} = W_1(\xi) \cdot \begin{bmatrix} N_e^2 - \kappa(c) \\ \dfrac{\kappa(c)\gamma_1(\xi)}{N_e} \\ 0 \end{bmatrix} \tag{6}$$

and

$$\Gamma_{i4} = W_1(\xi) \cdot \begin{bmatrix} 0 \\ N_e \\ \gamma_1(\xi) \\ N_e^2 - \kappa(c) \end{bmatrix}, \tag{7}$$

where $\kappa(c)$ is the dielectric constant in the cladding, and

$$\left. \begin{array}{l} \xi = [N_e^2 - \kappa(c)]^{1/2}\rho_i \\ W_1(\xi) = K_1(\xi)/[N_e^2 - \kappa(c)] \\ \gamma_1(\xi) = \xi \cdot K_1'(\xi)/K_1(\xi) \end{array} \right\}, \tag{8}$$

where K_1 is a modified Bessel function of the second kind and its prime denotes differentiation with respect to ξ. (Note that ρ_i is the value of ρ at the interface.)

The total solution Γ can be written in the core and cladding region separately.

In the core region, Γ is expressed by

$$\Gamma = A_1\Gamma_{i1} + A_2\Gamma_{i2}, \tag{9}$$

and in the cladding, Γ is expressed by

$$\Gamma = A_3\Gamma_{i3} + A_4\Gamma_{i4}, \tag{10}$$

where A_j is an arbitrary constant, $j = 1, 2, 3, 4$.

To calculate the field function Γ, we require basically four input data, namely, λ, the optimum core radius a_{opt}, N_e, and N. Among those parameters, calculation of N_e has been described in detail in Ref. 1. The material dispersion effect is incorporated with Maxwell's equations to achieve a high degree of accuracy for N_e. This is needed to acquire the precise eigenfunctions from eqs. 9 and 10.

In the design of a single-mode fiber, Δ is usually specified as an input data. It is rather small, ranging from 0.002 to 0.008, since the cladding of the fiber is generally made of a high-silica glass. The dispersive character of the cladding is well known.[9] Therefore, for a given Δ, the index of the core center N_1 can be expressed in terms of N_2 by

$$N_1 = \frac{N_2}{(1 - \Delta)}. \tag{11}$$

The dispersive properties of the N_2 in eq. (11) can be described by a modified Sellmeier formula.[1,7]

$$N_2 = C_0 + C_1\lambda^2 + C_2\lambda^4 + \frac{C_3}{(\lambda^2 - l)} + \frac{C_4}{(\lambda^2 - l)^2} + \frac{C_5}{(\lambda^2 - l)^3}, \quad (12)$$

where $l = 0.035$. The coefficients C_i are given in our previous work.[7]

For the index profile, we use a well-known formula that is particularly useful in fiber design.

$$N = N_1\left[1 - \Delta\left(\frac{R}{a}\right)^\alpha\right]. \quad (13)$$

Finally, the dispersion of the index N will be determined by substituting N_1 in eq. (13) with eqs. (11) and (12).

At the core-cladding interface, Γ must satisfy the continuity condition of the tangential field components. Consequently, this yields a set of simultaneous equations

$$\left.\begin{aligned}
A_1\Gamma_{11} + A_2\Gamma_{12} &= A_3\Gamma_{13} + A_4\Gamma_{14} \\
A_1\Gamma_{21} + A_2\Gamma_{22} &= A_3\Gamma_{23} + A_4\Gamma_{24} \\
A_1\Gamma_{31} + A_2\Gamma_{32} &= A_3\Gamma_{33} + A_4\Gamma_{34} \\
A_1\Gamma_{41} + A_2\Gamma_{42} &= A_3\Gamma_{43} + A_4\Gamma_{44}
\end{aligned}\right\}. \quad (14)$$

To compare the field distributions, it is convenient to introduce the following normalized variables into eq. (5).

$$\left.\begin{aligned}
\bar{E}_z &= \frac{E_z}{E_\phi(0)} \\
\bar{E}_\phi &= \frac{E_\phi}{E_\phi(0)} \\
\bar{E}_R &= \frac{E_R}{E_R(0)}
\end{aligned}\right\}, \quad (15)$$

$$\left.\begin{aligned}
\bar{H}_z &= \frac{H_z}{H_\phi(0)} \\
\bar{H}_\phi &= \frac{H_\phi}{H_\phi(0)} \\
\bar{H}_R &= \frac{H_R}{|H_R(0)|}
\end{aligned}\right\}. \quad (16)$$

III. ELECTROMAGNETIC FIELDS FOR THE HE$_{11}$ MODE IN DISPERSIONLESS SINGLE-MODE LIGHTGUIDES

We begin our study by considering a germania-doped silica lightguide with $\Delta = 0.002$ and $\lambda = 1.33\ \mu$m. The profile parameters examined are $\alpha = 100, 2,$ and 1. Thus, we span the range from rectangular through parabolic to triangular index functions. In Table I we calculate the values for the radii to make these lightguides dispersion-free.

Table I—Radii values for
dispersion-free lightguides

α	$a_{opt(\mu m)}$
100	4.142
2	5.725
1	6.294

The normalized electromagnetic fields as a function of normalized radii for these three cases are shown in Figs. 2a, 2b, and 2c. Note that in all cases the z fields are much smaller than the other field components. In fact, these fields are less than 3 percent of the tangential fields. The magnitude of the R and ϕ components of the electric and magnetic fields for a given α are all essentially the same. This is not likely if the index profile becomes more complex. For example, a profile
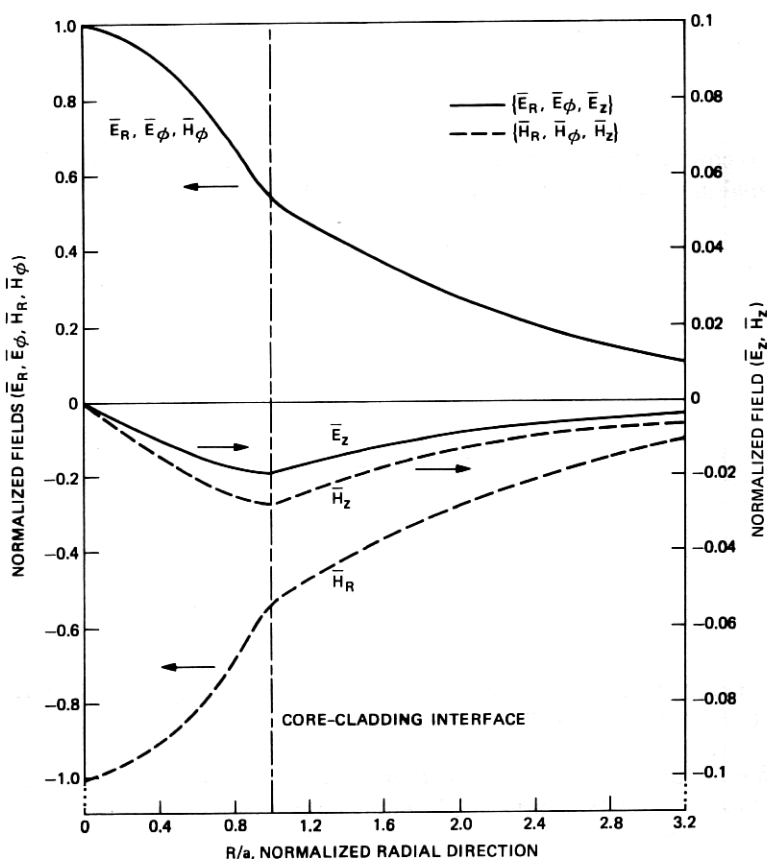
Fig. 2a—Normalized field distributions of the HE_{11} mode in a single-mode lightguide, where $\Delta = 0.002$, $\lambda = 1.33\ \mu m$, $\alpha = 100$, and $a_{opt} = 4.142\ \mu m$.

containing a central "burn out" and ripples, which would be characteristic of modified chemical vapor deposition (MCVD) profiles, would not have such a simple relationship between field components.

An interesting observation from Fig. 2 is that the slopes of the field components at the core-cladding interface change with α. For $\alpha = 100$, the field distribution near the interface forms a cusp, but it rounds progressively as α decreases. This is due solely to the index distribution in the core of the single-mode fiber.

Figure 3 shows the normalized transverse components of the electromagnetic field as a function of radial distance for the three α values. The curves are essentially identical up to $R = 3$ μm. However, beyond that distance they deviate appreciably. Also shown, by the vertical lines, are the optimum radii.
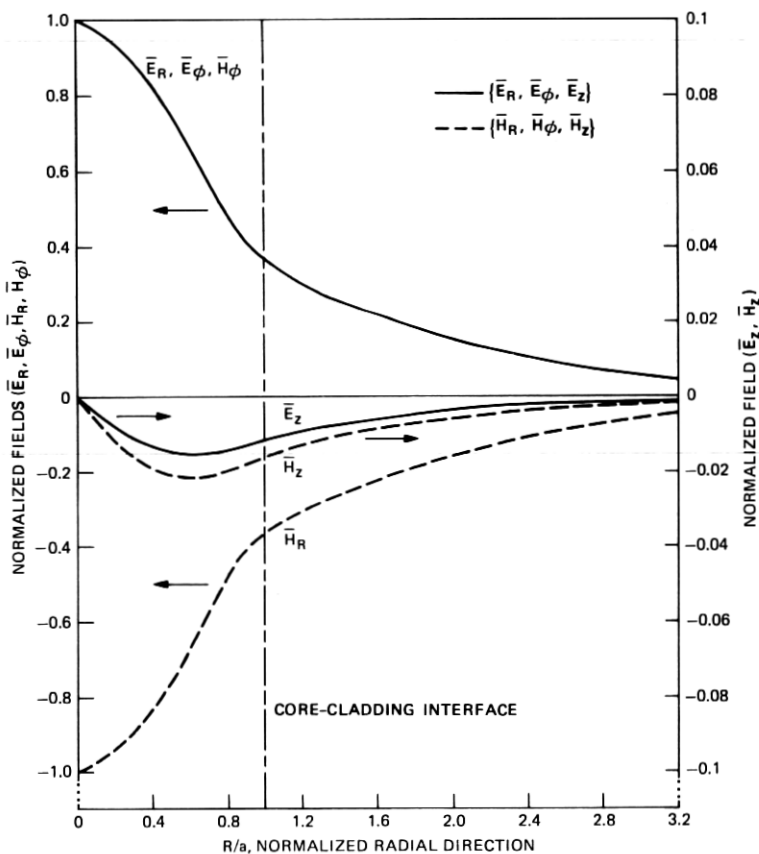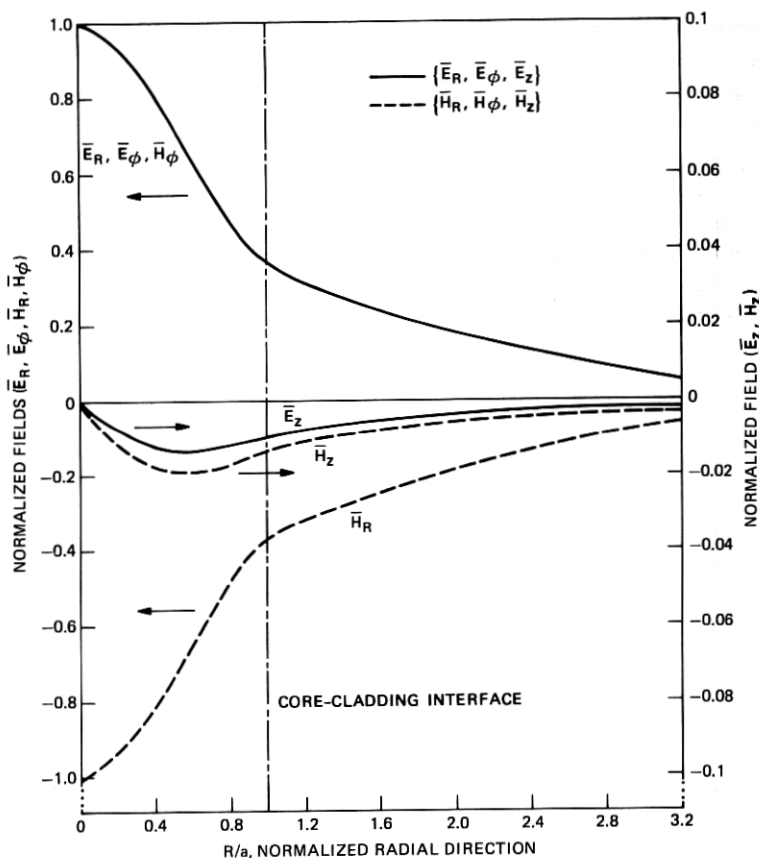

Fig. 2b—Normalized field distributions of the HE_{11} mode in a single-mode lightguide, where $\Delta = 0.002$, $\lambda = 1.33$ μm, $\alpha = 2$, and $a_{opt} = 5.725$ μm.

Fig. 2c—Normalized field distributions of the HE_{11} mode in a single-mode lightguide, where $\Delta = 0.002$, $\lambda = 1.33$ μm, $\alpha = 1$, and $a_{opt} = 6.294$ μm.

IV. ENERGY FLOW FOR THE HE_{11} MODE IN DISPERSIONLESS SINGLE-MODE LIGHTGUIDES

So far we have only considered the field in the fiber. However, in experimental practice it is more convenient to know the field intensity, which is the amount of energy flowing through the cross-section of the fiber. This can be calculated from the Poynting vector S in Ws/cm^2. The Poynting vector in the z direction, S_z is given by,

$$S_z = \tfrac{1}{2}(E_R H_\phi^* - E_\phi H_R^*), \tag{17}$$

where * indicates the complex conjugate of the variable.

We define the normalized Poynting vector I by

$$I = S_z/S_z(0). \tag{18}$$

Figure 4 shows the curves of I versus the normalized radial coordinate

R/a for three different α values. The normalized Poynting vector (field intensity) falls off more rapidly with normalized radius for lower α values.[10] As in Section III, when $\alpha = 100$ the Poynting vector develops a cusp at the core-cladding interface. We also note a near identity of the $\alpha = 1$ and $\alpha = 2$ curves. Thus, these two have nearly the same focusing power.

V. DEGREE OF FIELD CONFINEMENT

We know that the degree of field confinement in a fiber is related to its microbending loss.[4,5] In the fabrication of single-mode fiber cables for undersea applications, microbending loss has been one of the factors that determines the performance of the cable.
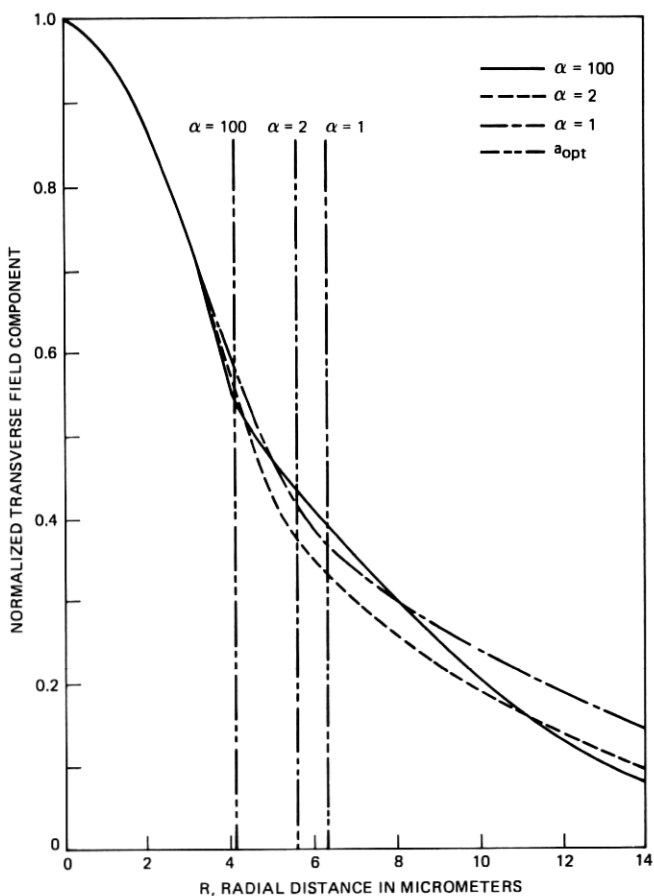

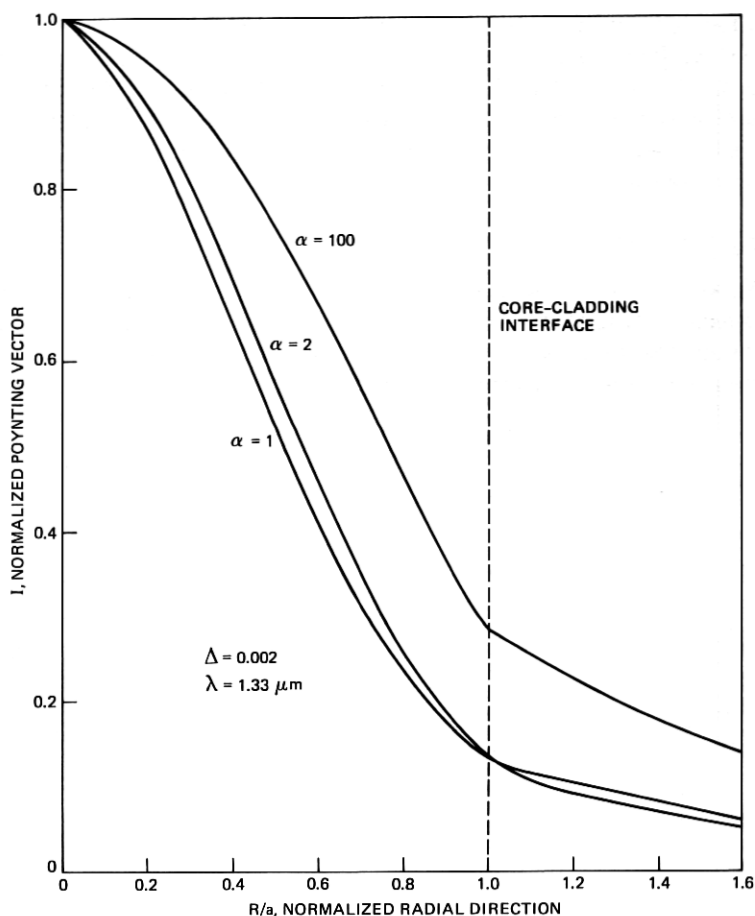Fig. 3—Normalized field components versus radial distance for three different values of α.

Fig. 4—Normalized Poynting vector versus normalized radial coordinate for three different values of α.

Figures 3 and 4 indicate that the field or power distribution is largely dependent on the index profile. To quantify the focusing power or confinement of a lightguide, we introduce a parameter Φ defined by:

$$\Phi = \frac{\displaystyle\int_0^{a_{\text{opt}}} S_z R dR}{\displaystyle\int_0^{\infty} S_z R dR}. \tag{19}$$

The parameter Φ represents the degree of power confined to the core with respect to the total propagating power. This ratio is plotted in Fig. 5, along with a_{opt}, as a function of α. We see that a_{opt} increases

with decreasing α and that Φ reaches its peak very near $\alpha = 2$. A slightly larger value for Φ occurs if the profile is Gaussian; that is,

$$N = N_1 \exp\left[-\left\{ \ln\left(\frac{N_1}{N_2}\right) \right\} \cdot \left(\frac{R}{a}\right)^2 \right]. \tag{20}$$

This value of Φ is the open circle in Fig. 5. We suspect that this slightly larger value may be caused by the close matching of the field with the index profile. The Gaussian index profile and the $\alpha = 2$ profile yield ~40 percent increase in Φ over the step-index profile case. This may help in eliminating microbending loss in single-mode fibers without increasing Δ.

VI. CORE-TO-CLAD RATIO

In the design and fabrication of single-mode lightguides, it is customary to fix the core-to-clad ratio at 0.1. This value seems appropriate for step-index fibers. It is, therefore, quite important to investigate the behavior of the evanescent field for graded-index fibers. From eqs. 6 and 7, we can readily calculate the field intensity in the cladding for different values of α and any radius.

For the cases of $\alpha = 100$, 2, and 1, including a Gaussian index profile,
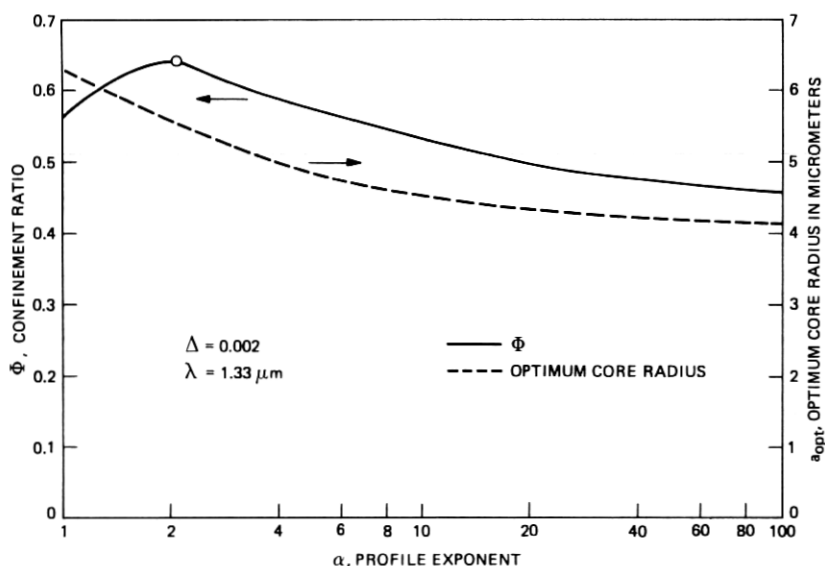

Fig. 5—Degree of field confinement in a single-mode fiber versus profile exponent α, (solid line). The dotted line shows the optimum core radius corresponding to the α value. The open circle indicates the maximum value of Φ obtained from a Gaussian-like index profile.
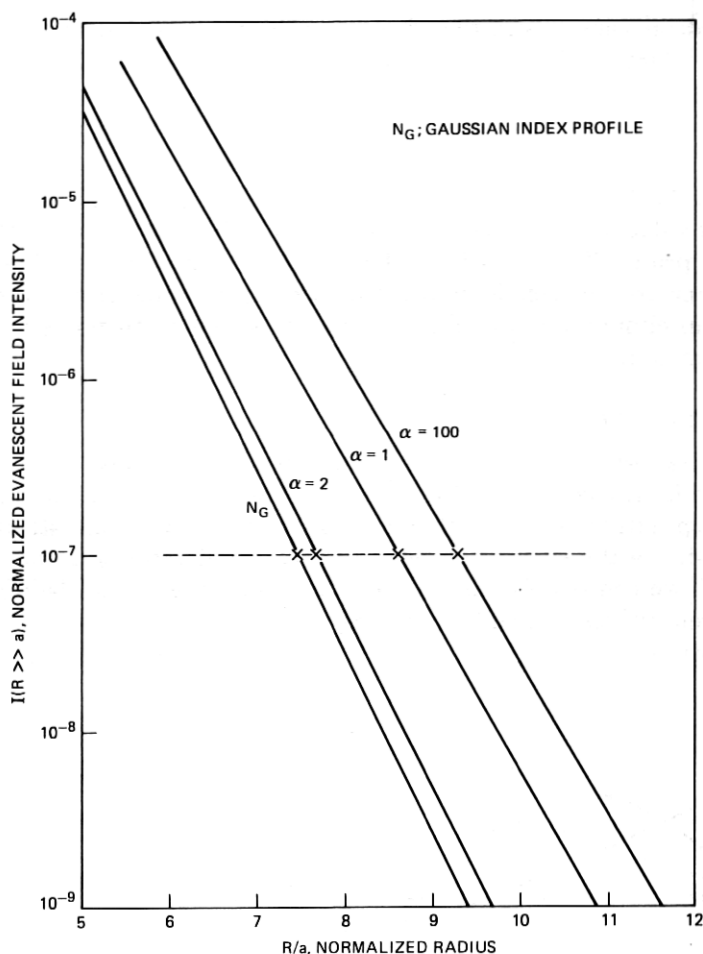
Fig. 6—Normalized evanescent field intensity at $R \gg a$ versus normalized radius for three different values of α and a Gaussian index profile. The horizontal dotted line is the cutoff level at $I = 10^{-7}$.

the results are given in Fig. 6. To compare the core-to-clad ratios for different α's we define an intensity level I at $R \gg a$ equal to 10^{-7} as the cutoff point. This corresponds to $R/a \sim 9.3$ for $\alpha = 100$. Accordingly, Fig. 6 shows that there are substantial differences in those values among the four cases. The clad-to-core ratio is reduced to 7.6 from 9.3 as α decreases to 2. The value for the Gaussian profile is very close to that for $\alpha = 2$. Finally, it is interesting to note that the value of I at the core-cladding interface is ~ 0.13 for $\alpha = 1$ and 2, but it is ~ 0.28 for $\alpha = 100$ (see Fig. 4).

VII. VALIDITY OF GAUSSIAN APPROXIMATION FOR THE FIELD FUNCTIONS OF HE₁₁ MODE

As mentioned earlier, it is usually not possible to find an analytical expression for the electromagnetic field functions for the HE_{11} mode in a single-mode fiber. One exception to this is the step-index profile. Therefore, an approximate expression for the field distribution of the fundamental mode is frequently used to determine the propagation characteristics. A prevailing approximation is a Gaussian-like field.[11,12,13] Thus, we can write

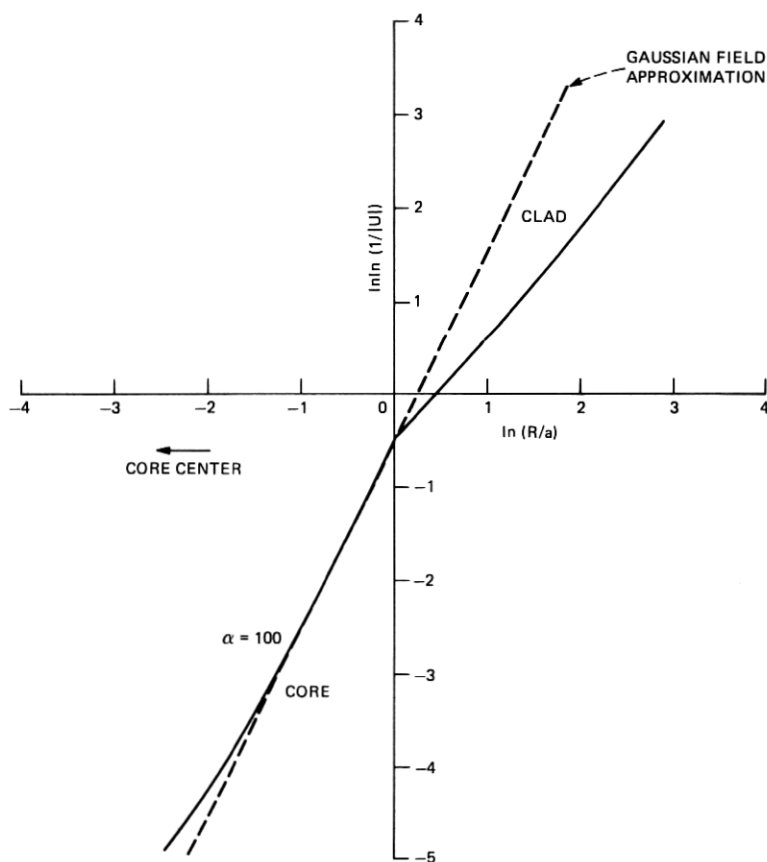$$E_g = E_0 \exp\left[-b \left(\frac{R}{a} \right)^m \right],$$
(21)

Fig. 7a—Comparison of Gaussian field distribution with exact field solutions. The solid lines are the exact values, and the dotted lines are the Gaussian approximation for $m = 2$ and $\alpha = 100$.

where E_0 and b are constants. Taking a double logarithm of both sides of eq. 21, we can rewrite it as

$$\ln \ln\left(\frac{1}{\bar{E}_g}\right) = \ln b + m \ln\left(\frac{R}{a}\right), \tag{22}$$

where

$$\bar{E}_g = E_g/E_0.$$

We introduce the dimensionless quantity U to represent any one of transverse electric or magnetic field components, for example, $\bar{E}_R$.

Equation (22) was plotted with $m = 2$ (precisely Gaussian) and compared with the exact values. The results are shown in Figs. 7a, b, and c for cases $\alpha = 100$, 2, and 1. The solid lines are the exact values, while the dotted lines are from the Gaussian approximation. In all
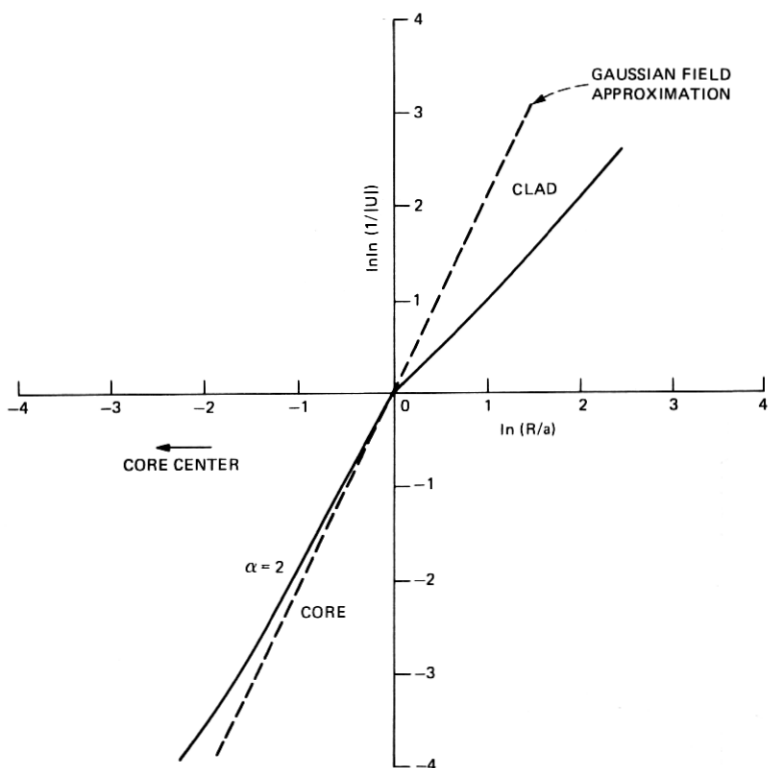

Fig. 7b—Comparison of Gaussian field distribution with exact field solutions. The solid lines are the exact values and the dotted lines are the Gaussian approximation for $m = 2$ and $\alpha = 2$.
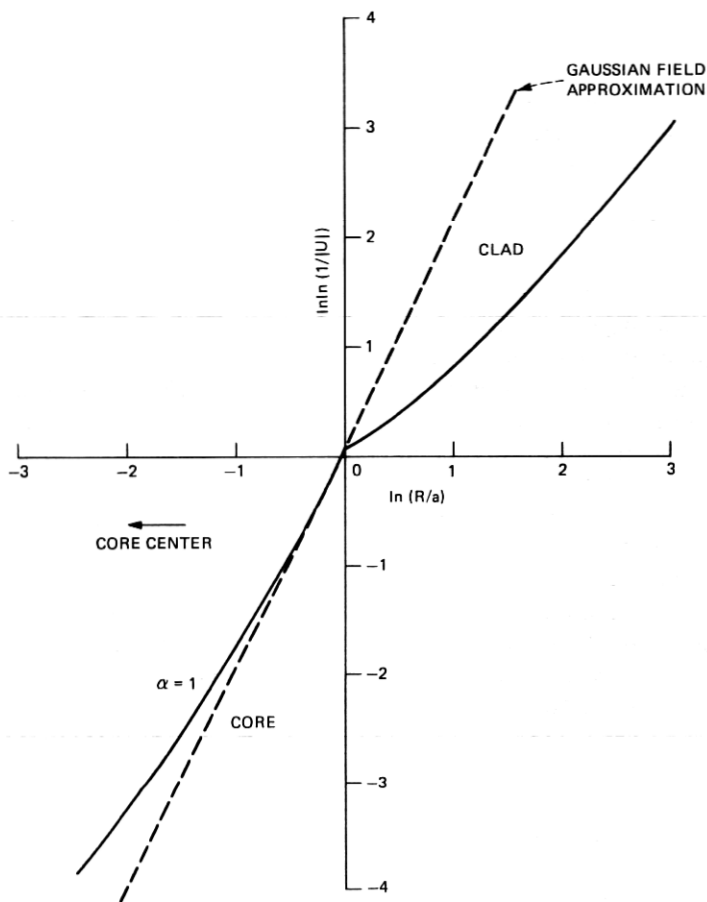
Fig. 7c—Comparison of Gaussian field distribution with exact field solutions. The solid lines are the exact values, and the dotted lines are the Gaussian approximation for $m = 2$ and $\alpha = 1$.

cases, the fields of the core region appear in the third quadrant of the figures. Those in the cladding region are shown in the first quadrant.

For the core region, when $\alpha = 100$ and it is near the core-cladding interface, there is satisfactory agreement between the Gaussian field function and the exact field function. There is poor agreement near the center of the core; this is also evident from Refs. 11 and 12. When $\alpha = 2$ or 1 there is much worse agreement between the exact and Gaussian functions in the core regions. For all values of α, the agreement in the cladding region is extremely poor. It is interesting to note that the slope of the exact field functions in the cladding for all α values is close to 1. This indicates that the field is decaying exponentially.

VIII. SUMMARY AND CONCLUSIONS

From a numerical solution to Maxwell's equations, we can accurately describe the field distribution of the HE_{11} mode in a single-mode lightguide. According to our calculated results, the fraction of power in the core reaches its maximum value near $\alpha = 2$. Thus, for a parabolic profile or Gaussian profile, the fraction of power within the core is ~40 percent larger than that of a step-index core. On the other hand, it is clear that the optimum core size increases with decreasing α value. A linear index profile ($\alpha = 1$) provides an optimum core size that is over 50 percent larger than that of a step-index core. Therefore, in designing a single-mode fiber, it is important to remember that one should choose a value of α to optimize certain characteristics, such as zero total dispersion, TE and TM cutoff, core size, manufacturing tolerances, field confinement, or microbending loss.

The work of Marcuse shows that for the case of step-index, single-mode fibers, microbending losses can either increase or decrease as a function of fiber radius, depending upon the statistics of the axis deformation function.[14,15,16] He also concludes that single-mode fibers with parabolic-index profiles may have smaller microbending losses than single-mode, step-index fibers. If the distortion power spectrum peaks sharply at low spatial frequencies, the advantage will be slight, if it exists at all. However, for distortions with a wider Fourier spectrum, the parabolic-index fiber should clearly be advantageous. The reason for this is that in the case of the distorted parabolic-index fiber, the sources of the radiation field are distributed throughout its volume, while in the case of the step-index fiber, they are located at the waveguide boundary. The constructive interference among the volume sources is never as pronounced as among the boundary sources.

It should be noted that when we increase the mode confinement we reduce the field at the core-cladding interface. This reduces the strength of the radiation sources because of microbending at this boundary. Furthermore, if there is a barrier layer such as B_2O_3, then bulk loss is reduced as well.

An additional discussion seems in order concerning the important TE and TM cutoff. As we have previously shown[1] for $\Delta = .002$ and $\lambda = 1.33$ μm, the TE and TM cutoff is 1.0 μm when $\alpha = 100$, and it shifts to 0.85 μm for $\alpha = 1$. Attempts to increase the field confinement by increasing Δ, while keeping the core radius fixed, may move the cutoff rather close to the operating wavelength. Instead of increasing Δ it may sometimes be better to reduce α. The substantial increase in core size when $\alpha = 2$ is an advantage as far as coupling to a source is concerned. It has the important added advantage in that the clad-to-core ratio is reduced.

Finally, we must conclude that the Gaussian field approximation is

likely to be of value only in the core region of a step-index fiber. It is always very poor in the cladding. However, the Gaussian-like approximation with $m \neq 2$ may be useful for graded-index, single-mode lightguides. For example, for $\alpha = 1$ and 2 the m values for best fit are ~ 1.6 and ~ 1.8, respectively.

IX. ACKNOWLEDGMENTS

REFERENCES

1. U. C. Paek, G. E. Peterson, and A. Carnevale, "Dispersionless Single-mode Lightguides with α Index Profiles," B.S.T.J. *60*, No. 5 (May–June 1981), pp. 583–98.
2. L. G. Cohen, C. Lin, and W. G. French, "Tailoring Zero Chromatic Dispersion into the 1.5-1.6 μm Low-Loss Spectral Region of Single-Mode Fibers," Electron. Lett., *15* (June 1979), pp. 334–5.
3. W. A. Gambling, H. Matsumura, and C. M. Ragdale, "Zero Total Dispersion in Graded-Index Single Mode Fibers," Electron. Lett., *15* (July 1979), pp. 474–6.
4. J. Sakai and T. Kimura, "Practical Microbending Loss Formula for Single-Mode Optical Fibers," IEEE J. Quantum Electron., *QE-15* (June 1979), pp. 497–500.
5. J. Sakai, "Simplified Bending Loss Formula for Single-Mode Optical Fiber," Appl. Opt., *18* (April 1979), pp. 951–2.
6. T. Li, "Structures, Parameters and Transmission Properties of Optical Fibers," Proc. IEEE, *68* (October 1980), pp. 1175–80.
7. G. E. Peterson et al., "An Exact Numerical Solution to Maxwell's Equations for Lightguides," BSTJ, *59* (September 1980), pp. 1175–96.
8. M. O. Vassel, "Calculation of Propagating Modes in a Graded-Index Optical Fiber," Opto-Electronics, *5* (July 1974), pp. 271–386.
9. J. W. Fleming, "Material Dispersion in Lightguide Glasses," Electron. Lett., *14* (May 1978), pp. 326–8.
10. W. A. Gambling and H. Matsumura, "Propagation in Radially-Inhomogenous Single Mode Fiber," Opt. Quantum Electron., *10* (January 1978), pp. 31–40.
11. D. Marcuse, "Gaussian Approximation of the Fundamental Modes of Graded-Index Fibers," J. Opt. Soc. Am., *68* (January 1978), pp. 103–9.
12. A. W. Snyder and R. A. Sammut, "Fundamental HE_{11} Modes of Graded Optical Fibers," J. Opt. Soc. Am., *69* (December 1979), pp. 1663–71.
13. H. Matsumura and T. Suganuma, "Normalization of Single-Mode Fibers Having an Arbituary Profile," Appl. Opt., *19* (September 1980), pp. 3151–8.
14. D. Marcuse, "Microbending Losses of Single-Mode, Step-Index and Multimode Parabolic-Index Fibers," B.S.T.J. *55*, No. 7 (September 1976), pp. 937–55.
15. D. Marcuse, "Theory of Dielectric Optical Waveguides," New York: Academic Press, 1974.
16. D. Marcuse, "Radiation Losses of Parabolic-Index Slabs and Fibers with Bent Axes," Appl. Opt., *17* (March 1978), pp. 755–62.